Available online at www.sciencedirect.com
ScienceDirect
Biochimica et Biophysica Acta 1778 (2008) 835–843
Biochimica et Biophysica Acta BBA
www.elsevier.com/locate/bbamem

Stabilization of Na,K–ATPase by ionic interactions

Elfrieda Fodor [a], Natalya U. Fedosova [b], Csilla Ferencz [a], Derek Marsh [c], Tibor Pali [a], Mikael Esmann [b,*]

[a] *Institute of Biophysics, Biological Research Centre, Szeged, Hungary*
[b] *Institute of Physiology and Biophysics, Ole Worms Allé 1185, University of Aarhus, DK-8000 Aarhus, Denmark*
[c] *Max-Planck-Institut für biophysikalische Chemie, Abt. Spektroskopie, 37070 Göttingen, Germany*

Received 2 May 2007; received in revised form 26 September 2007; accepted 10 December 2007
Available online 15 December 2007

Abstract

The effect of ions on the thermostability and unfolding of Na,K–ATPase from shark salt gland was studied and compared with that of Na,K–ATPase from pig kidney by using differential scanning calorimetry (DSC) and activity assays. In 1 mM histidine at pH 7, the shark enzyme inactivates rapidly at 20 °C, as does the kidney enzyme at 42 °C (but not at 20 °C). Increasing ionic strength by addition of 20 mM histidine, or of 1 mM NaCl or KCl, protects both enzymes against this rapid inactivation. As detected by DSC, the shark enzyme undergoes thermal unfolding at lower temperature ($T_m \approx 45$ °C) than does the kidney enzyme ($T_m \approx 55$ °C). Both calorimetric endotherms indicate multi-step unfolding, probably associated with different cooperative domains. Whereas the overall heat of unfolding is similar for the kidney enzyme in either 1 mM or 20 mM histidine, components with high mid-point temperatures are lost from the unfolding transition of the shark enzyme in 1 mM histidine, relative to that in 20 mM histidine. This is attributed to partial unfolding of the enzyme due to a high hydrostatic pressure during centrifugation of DSC samples at low ionic strength, which correlates with inactivation measurements. Addition of 10 mM NaCl to shark enzyme in 1 mM histidine protects against inactivation during centrifugation of the DSC sample, but incubation for 1 h at 20 °C prior to addition of NaCl results in loss of components with lower mid-point temperatures within the unfolding transition. Cations at millimolar concentration therefore afford at least two distinct modes of stabilization, likely affecting separate cooperative domains. The different thermal stabilities and denaturation temperatures of the two Na,K–ATPases correlate with the respective physiological temperatures, and may be attributed to the different lipid environments.

Keywords: Na,K–ATPase; Denaturation; Pig kidney; Shark salt gland; Differential scanning calorimetry; Electrostatic screening

1. Introduction

Na,K–ATPase, an extensively studied member of the P-type ATPase family, is involved in regulation of cell volume, development of membrane potential, and transport of nutrients and water in animal tissues [1]. It is an oligomeric complex, where the α-subunit carries out ion transport coupled to ATP hydrolysis, the β-subunit is mostly a chaperone responsible for correct membrane insertion, and the γ-subunit (an FXYD-protein) modulates transport activities of the enzyme by affecting the apparent affinities for cations [2]. The three-dimensional organization of Na,K–ATPase at atomic resolution is not yet known, and for this reason the structure of the homologous enzyme, Ca–ATPase (SERCA 1a), is widely used for interpretation of results on the former [3]. This is justified because the sequence of the Na,K–ATPase α-subunit is highly homologous to that of the Ca–ATPase, with only minor gaps and insertions. Additionally, a 3-D model of pig kidney Na,K–ATPase αβγ protomer, based on cryo-electron microscopy of two-dimensional crystals, reveals distinct similarities between the catalytic α-subunit and the Ca–ATPase, given the predicted locations of the β- and γ-subunits in Na,K–ATPase [4].

Abbreviations: CDTA, *trans*-1,2-cyclohexylenedinitrilo-tetraacetic acid; $E_2(K)$, the protein conformation in the presence of K^+; SDS, sodium dodecyl sulphate; DSC, differential scanning calorimetry

* Corresponding author. Tel.: +45 8942 2930; fax: +45 8612 9599.
E-mail address: me@biophys.au.dk (M. Esmann).

0005-2736/$ - see front matter © 2007 Elsevier B.V. All rights reserved.
doi:10.1016/j.bbamem.2007.12.006

According to current structural classifications, the catalytic subunit of a P-type ATPase consists of four well-defined domains: a membrane-bound domain, extra-membranous domains involved in phosphorylation (P) or in nucleotide binding (N), and the extra-membranous hinge domain (A). Many members of the P-type ATPase family contain additional subunits that may be considered as separate domains in the overall structure of the enzyme. For the Na,K–ATPase, the two additional subunits β and γ each have a single transmembrane span. Differential scanning calorimetry (DSC) experiments with P-type ATPases, on the other hand, have been interpreted in terms of the unfolding of a smaller number of independent cooperative domains: two for the α-protomer Ca–ATPase [5] and the αβ-protomer gastric H,K–ATPase [6], and three for the αβγ-protomer renal Na,K–ATPase [7].

The common architecture of P-type ATPases implies a common mechanism of action. Transport of ions against their electrochemical gradients is coupled to ATP hydrolysis, and this coupling occurs through a conformational change (E_1–E_2) of the enzyme molecule. Differences between these two major conformations have been characterized by various methods (see Refs. [1,8] for reviews), and recently visualized in crystal structures of the Ca–ATPase [3,9]. The most profound changes are in the relative positions of the extra-membranous domains. For renal Na,K–ATPase, the E_2(K)-form (in 20 mM K^+) is more stable towards thermal denaturation than is the E_1-form (in 20 mM Na^+) [10,11]. Induction of the E_2-conformer by 10 mM Rb^+ (a congener of K^+) similarly affords protection against inactivation and trypsinolysis on incubation at 55 °C [12,13], a temperature at which thermal unfolding would otherwise occur.

To study the effect of cations and ionic strength on the stability, and the number of independent cooperative domains in the thermal unfolding of these enzymes we have chosen two almost identical proteins that function at different temperatures. In the present study, we characterize the effects of ionic strength and low concentrations of cations on the thermostability and thermal unfolding of Na,K–ATPase from tissues of different organisms: shark salt gland and pig kidney. These animals belong to the poikilotherms and homeotherms, respectively, and therefore the Na,K–ATPases are adapted to function at different temperatures (about 8 °C for shark and 36 °C for pig). Thermal unfolding [14], and inactivation at low ionic strength, take place at lower temperatures for shark salt gland Na,K–ATPase than for the enzyme from pig kidney. Protection of both shark and pig kidney Na,K–ATPases from inactivation at low ionic strength is afforded by a variety of cations at millimolar concentration. Na^+, $Tris^+$, choline and protonated histidine are equally effective and protection appears to follow a simple Debye–Hückel dependence on ionic strength, whereas K^+ is more efficient, presumably due to induction of the E_2(K)-form. Inactivation of shark Na,K–ATPase at low ionic strength, either thermally or as a result of high-speed centrifugation [15], correlates with the pattern of multi-step thermal unfolding at higher temperatures. Centrifugation at low temperature selectively removes calorimetric components at higher temperatures within the unfolding transition, whereas incubation at increased temperature removes components at lower temperatures within the transition. Again protection is afforded by increasing the ionic strength.

2. Materials and methods

2.1. Enzyme preparation

Na,K–ATPase from the salt gland of *Squalus acanthias* was prepared according to the method of Skou and Esmann [16], omitting the saponin treatment. Na,K–ATPase from pig kidney microsomal membranes was prepared by treatment with SDS and purified by differential centrifugation [17,18]. The specific activity of both enzyme preparations was approximately 30 μmol ATP hydrolysed/mg protein per min at 37 °C [19].

2.2. Stability measurements

The purified membrane preparation (stored at 5 mg protein/mL) was diluted into buffer solution containing 1 or 20 mM histidine (neutralized to pH 7.0 with CDTA at the given temperature), with or without additional salt, to a final concentration of 0.1 mg/mL and incubated for up to 3 h at different temperatures. The cation concentration of 1 mM histidine at pH 7 is calculated to be 0.1 mM (pK_a=6.05 for histidine imidazole), which is neutralized by 0.03 mM of trivalent CDTA. Steady-state Na,K–ATPase activities were assayed at the time points shown in Figs. 1 and 2 by a 10-fold dilution of protein into an assay medium containing 130 mM NaCl, 20 mM KCl, 4 mM $MgCl_2$ and 3 mM ATP, with or without 1 mM ouabain, at 20 °C. Phosphate liberation after 2–6 min was measured colorimetrically [20].

2.3. Sample preparation for differential scanning calorimetry

Purified membrane preparations were diluted with 1 or 20 mM histidine (pH 7.0 at 20 °C) to a final concentration of ca. 0.1 mg/mL. The sample was either incubated for 1 h at 20 °C and centrifuged at 4 °C for 2 h (20000 rpm in a Beckman Ti70 rotor, average g=29.400) or immediately subjected to centrifugation for 2 h at 4 °C. The pellet was resuspended in the same buffer (at a protein concentration of ca. 2.4 mg/mL) and used for DSC experiments.

2.4. Differential scanning calorimetry

DSC measurements were performed using a VP-DSC calorimeter, with 0.5-mL sample and reference cells, from MicroCal, LLC (Northampton, MA). The instrumental baseline was determined before each sample scan, by filling both sample and reference cells with the buffer used for the membrane samples, and using the same scanning parameters. Samples were scanned between 5 and 95 °C, at a rate of 1 K·min^{-1}, using the passive feedback mode of the VP-DSC instrument. Immediately after completion of the heating scan, a down-scan from 95 to 5 °C was

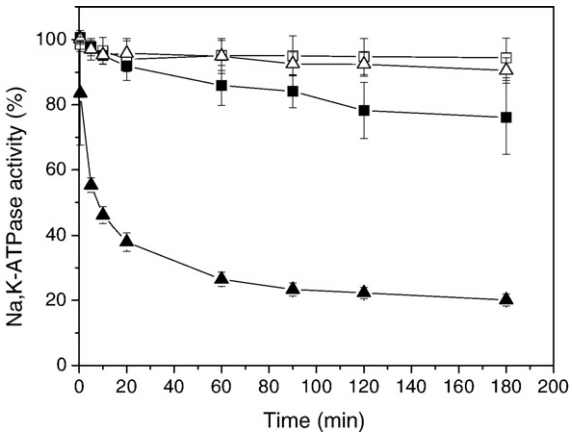

Fig. 1. Inactivation profiles for membranous Na,K–ATPase from shark salt gland. Membranes at a concentration of 0.1 mg protein/mL were incubated at different temperatures and under different ionic conditions: 1 mM histidine at 20 °C (▲);20 mM histidine at 20 °C (Δ); 1 mM histidine at 4 °C (■); and 20 mM histidine at 4 °C (□). 100% is the activity of a fully active enzyme preparation (see Methods), and averages±SD of three determinations are shown.

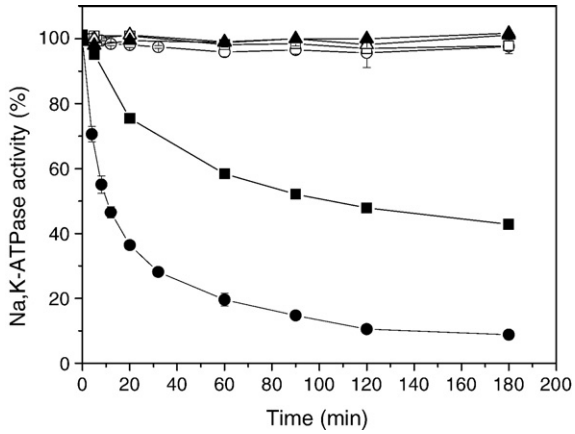

Fig. 2. Inactivation profiles for membranous Na,K–ATPase from pig kidney. Membranes at a concentration of 0.1 mg protein/mL were incubated at different temperatures and under different ionic conditions: 1 mM histidine at 20 °C (▲);20 mM histidine at 20 °C (Δ); 1 mM histidine at 40 °C (■); 20 mM histidine at 40 °C (□); 1 mM histidine at 42 °C (●); and 20 mM histidine at 42 °C (○). 100% is the activity of a fully active enzyme preparation (see Methods), and averages±SD of three determinations are shown.

performed at the same 1 K·min^{-1} rate. Reversibility and repeatability of the unfolding process was checked by the down-scan and a second up-scan, respectively. Before the start, and between repeated heating cycles, the samples were allowed to equilibrate for 30 min at 5 °C. The pH of the sample buffer (see Section 2.3) decreased from 7.0 at 20 °C to about 6.7 at 50 °C.

Heat capacity data were corrected for the instrument baseline, and normalized for scan rate and protein concentration. The enzyme concentration of the sample in the DSC cell was determined by measuring the total protein content [19] and a nucleotide binding site concentration of about 2.8 nmol per mg protein for both the shark and kidney enzyme preparations was used for normalization [Fedosova and Esmann, unpublished]. Excess heat capacity profiles were analyzed by using the Origin software provided with the instrument. A progress baseline was fitted to each profile and subtracted, by selecting appropriate pre- and post- transitional segments. The number of components present in the first unfolding endotherm, the heat of denaturation (ΔH_d) and the transition temperature (T_d) were estimated in each case by fitting the thermogram with components corresponding to independent two-state transitions. The number of components in the fitting procedure was kept at the minimum possible that resulted in a good fit to the data. Decreasing the number of components by one resulted in a large increase in the value of χ^2 for the fit, whereas adding a further component produced only a modest reduction in χ^2. For example, for the endotherm given later in Fig. 5, decreasing the number of fitting components from five to four increased χ^2 by a factor of 12× whereas increasing the number of components to six decreased χ^2 by only ~2×.

3. Results

3.1. Activity profiles of shark and kidney Na,K–ATPase

Fig. 1 shows the dependence of the activity of membranous shark salt gland Na,K–ATPase on time of incubation in 1 mM or 20 mM histidine, at either 4 °C or 20 °C. In 20 mM histidine, the shark enzyme is stable at both temperatures over a period of up to 3 h (only on incubation at 37 °C for 1 h, is the shark enzyme appreciably inactivated in 20 mM histidine). In 1 mM histidine, activity of the shark enzyme decreases steadily on incubation at 4 °C, and the inactivation becomes rapid on increasing the temperature to 20 °C.

Fig. 2 shows the time dependence of the activity of the pig kidney enzyme, when incubated under conditions similar to those of the shark enzyme in Fig. 1. Both in 1 mM histidine and in 20 mM histidine, the kidney enzyme is stable at 20 °C (as well as at 4 °C — not shown): the activity does not decrease over a period of 3 h at either temperature. Only on incubation at around 40 °C does the kidney enzyme begin to inactivate in 1 mM histidine. At 42 °C the rate of inactivation of the kidney enzyme is similar to that of the shark enzyme at 20 °C. In 20 mM histidine the kidney enzyme is stable both at 40 and at 42 °C. These latter results correlate with the difference in physiological temperatures of the shark and pig.

3.2. Salt- and cation-induced stabilization of shark and kidney Na,K–ATPase

The stabilizing effect is not unique to histidine, but can be induced by other ions. Fig. 3A shows the dependence of the residual activity of shark enzyme, after incubation for 20 min at 20 °C, on the concentration of NaCl or KCl in an incubation medium containing 1 mM histidine. Both NaCl and KCl at low concentrations are able to protect against inactivation, with half-maximal protection achieved at ca. 0.2 mM and 0.1 mM, respectively, and full protection at above 1 mM salt. This salt concentration is comparable to the ionic strength of a 20 mM

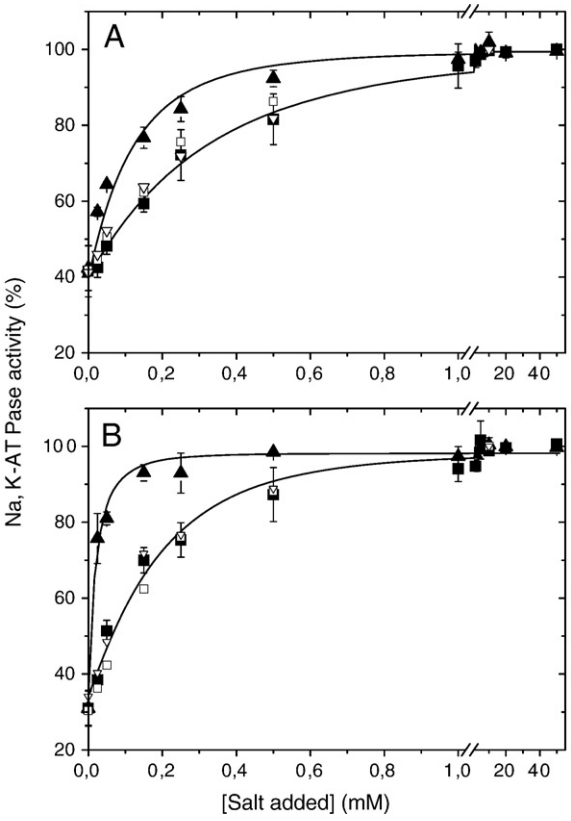

Fig. 3. Salt and cation protection against inactivation of Na,K–ATPase in 1 mM histidine. Panel A shows experiments with shark enzyme at 20 °C, and panel B experiments with pig kidney enzyme at 42 °C (both with 0.1 mg protein/mL). The activity remaining after incubation for 20 min is given as a function of the concentration of added NaCl (■), KCl (▲), TrisCl (□) or cholineCl (Δ). 100% is the activity of a fully active enzyme preparation (see Methods), and averages± SD of three determinations are shown. The full lines represent non-linear fitting of Eq. (2) or (3) to the data (see Discussion). The 1 mM histidine adjusted to pH 7.0 by CDTA contributes 0.185×10^{-3} M to the total ionic strength.

histidine buffer at pH 7.0, where approximately 10% of the histidine is protonated.

Fig. 3B shows a similar experiment with the pig kidney enzyme but at 42 °C, and the protective effect of NaCl is comparable to that for shark enzyme. For both enzymes, incubation in ≥1 mM salt protects against inactivation over a 3 h period (shark at 20 °C and kidney at 42 °C). The better protection offered by KCl than by NaCl is more pronounced with kidney enzyme than with shark enzyme.

Tris and choline (as chloride salts) protect both shark and kidney enzyme against inactivation with the same concentration dependence as that of NaCl (see Fig. 3). This indicates that the better protection by KCl is a specific effect (presumably induction of the E_2(K)-form), and that the identical protective effects of NaCl, TrisCl and cholineCl are due to electrostatic shielding effects, which can be described within the framework of Debye–Hückel theory (see Discussion).

3.3. Differential scanning calorimetry of shark membranes

Fig. 4 shows the DSC heating scans for membranous shark Na,K–ATPase preparations at different ionic strengths and under various preparation conditions. The four distinct protocols, which correspond to the four panels (A–D) of Fig. 4, were designed to test the factors affecting enzyme stability as established here by activity measurements and in a previous study on the effects of high-speed centrifugation [15]. Panel A corresponds to the control situation: the fully active enzyme is in 20 mM histidine and all preparation procedures, including centrifugation, were performed at 4 °C. Fig. 4A gives the first heating scan; for this and all other samples, the thermal denaturation is irreversible. Neither the cooling nor the reheating scans contained any transition peaks, and the post-transitional baselines at the end of the first heating scans showed no signs of sample aggregation. As seen from Fig. 4A, the thermal unfolding is not a simple single two-state transition; up to four components are required to fit the complete endotherm. Heats of unfolding and mid-point temperatures of the component peaks are listed in Table 1. The peak maximum of the overall endotherm is at 45 °C, but components with comparable heats of unfolding are present at 33, 41 and 50 °C.

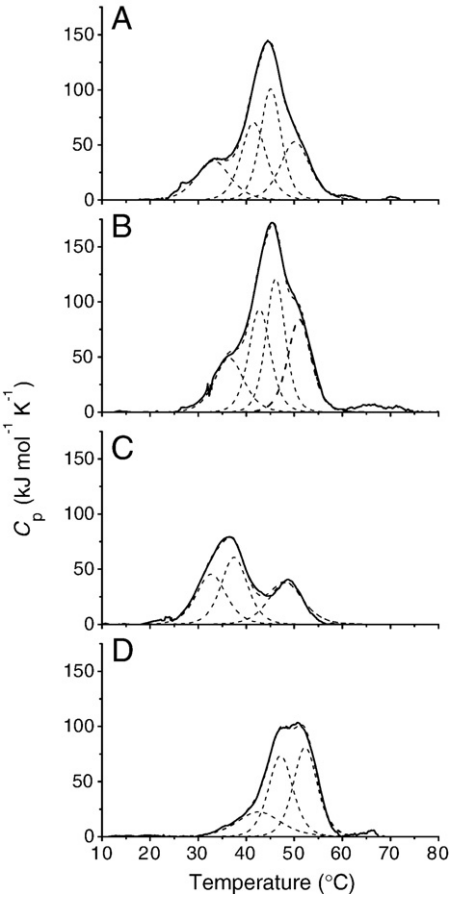

Fig. 4. Excess heat capacity functions of membranous Na,K–ATPase from shark salt gland, after baseline subtraction. (A) Enzyme in 20 mM histidine, centrifuged for 2 h at 4 °C. (B) Enzyme in 20 mM histidine, preincubated for 1 h at 20 °C, prior to centrifugation for 2 h at 4 °C. (C) Enzyme in 1 mM histidine, centrifuged for 2 h at 4 °C. (D) Enzyme in 1 mM histidine, preincubated for 1 h at 20 °C prior to addition of 10 mM NaCl and subsequent centrifugation for 2 h at 4 °C. Dashed lines represent fitted components.

Table 1
Mid-point temperatures, T_d, and heats of transition, ΔH_d, of the components fitting the calorimetric endotherms of membranous shark Na,K–ATPase

Condition	Activity (%)	T_m (°C)	T_d (°C)	ΔH_d (kJ·mol^{-1})	ΔH_{tot} (kJ·mol^{-1})
20 mM His	110±5	44.5	33.2	335	1830
no preincubation			41.5	482	
			45.1	582	
			50.2	431	
20 mM His	108±6	45.2	36.5	398	2140
preincubated 1 h at 20 °C			43.0	557	
			46.1	641	
			51.1	544	
1 mM His	64±8	36.4	32.8	377	1181
no preincubation			37.5	444	
			48.2	360	
1 mM His preincubated	27±4	50.7	42.7	272	1311
1 h at 20 °C, 10 mM			47.2	502	
NaCl added before			52.3	536	
centrifugation					

ΔH_{tot} and T_m are the heat of transition and the transition mid-point temperature of the entire endotherm. The ATPase activity is expressed as percentage of that of the native enzyme without incubation or centrifugation. Typical uncertainties arising from fitting are ±0.1° in T_d and ±4 kJ·mol^{-1} in ΔH_d. Root -mean-square deviations of the fits are typically 1–2% of the heat capacity maximum. Sample-to-sample variation in ΔH_{tot} was typically less than 4%.

Fig. 4B shows the first heating scan for shark enzyme in 20 mM histidine that was preincubated for 1 h at 20 °C prior to centrifugation at 4 °C. The shape of the endotherm is similar to that of the sample that was not preincubated at 20 °C, and the total enthalpy is similar to that of the control (see Table 1). This result correlates with the protection of the shark enzyme against inactivation that is afforded by 20 mM histidine (see Fig. 1).

Fig. 4C shows the first DSC heating scan for shark enzyme in 1 mM histidine that was kept at 4 °C during the sample preparation and not preincubated at higher temperature prior to centrifugation. The result is a considerable change in shape of the endotherm and reduction in overall heat of transition (see Table 1), relative to control enzyme in 20 mM histidine. Principally, heat is lost

from components of the control endotherm that occur at higher temperature (cf. Fig. 4A). This reduction in heat of unfolding correlates with the inactivation of the shark enzyme by centrifugation at low ionic strength [15], and also with the steady rate of inactivation on incubation in 1 mM histidine at 4 °C (see Fig. 1). Of the net 35% reduction in activity (see Table 1), up to ca. 15% could be attributed to centrifugation, because the enzyme is inactivated by approximately 20% simply during incubation at 4 °C for 2 h (see Fig. 1).

Addition of 10 mM NaCl protects against inactivation during centrifugation and Fig. 4D shows the first DSC heating scan of shark enzyme in 1 mM histidine that was preincubated for 1 h at 20 °C, but to which 10 mM NaCl was then added prior to centrifugation at 4 °C (note that NaCl was present during the centrifugation step only). Again, the shape of the calorimetric endotherm differs considerably from that of the control (Fig. 4A), but in a very different way from that of the enzyme in 1 mM histidine that was not preincubated but lacked NaCl in the centrifugation step (Fig. 4C). In this case (i.e., Fig. 4D), heat is lost from the components with lower mid-point temperatures in the control sample. This corresponds to the ca. 70% inactivation of the shark enzyme (see Table 1), which is accounted for completely by the incubation at 20 °C for 1 h in 1 mM histidine in the absence of NaCl (see Figs. 1 and 3).

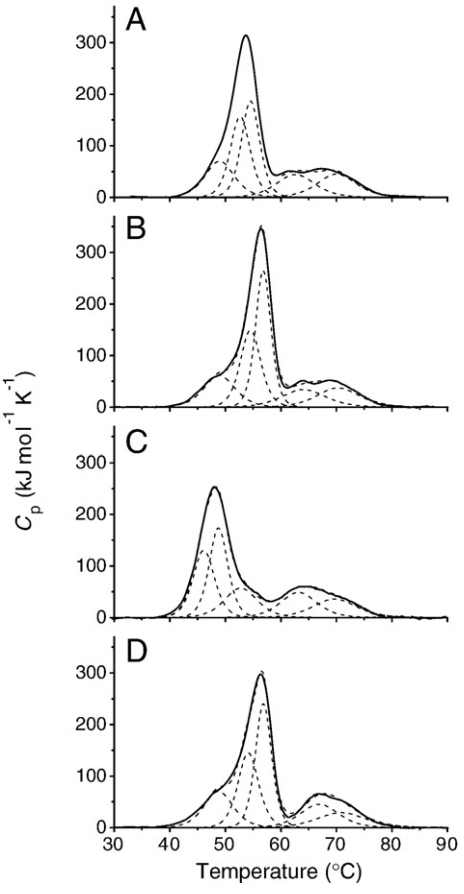

Fig. 5. Excess heat capacity functions of membranous Na,K–ATPase from pig kidney, after baseline subtraction. (A) Enzyme in 20 mM histidine, centrifuged for 2 h at 4 °C. (B) Enzyme in 20 mM histidine, preincubated for 1 h at 20 °C prior to centrifugation for 2 h at 4 °C. (C) Enzyme in 1 mM histidine, centrifuged for 2 h at 4 °C. (D) Enzyme in 1 mM histidine, preincubated for 1 h at 20 °C prior to addition of 10 mM NaCl and subsequent centrifugation for 2 h at 4 °C. Dashed lines represent fitted components.

Table 2
Mid-point temperatures, T_d, and heats of transition, ΔH_d, of the components fitting the calorimetric endotherms of membranous pig kidney Na,K–ATPase

Condition	Activity (%)	T_m (°C)	T_d (°C)	ΔH_d (kJ·mol^{-1})	ΔH_{tot} (kJ·mol^{-1})
20 mM His no preincubation	87±9	53.7	49.0	494	2889
			52.7	745	
			54.6	816	
			62.7	410	
			70.1	423	
20 mM His preincubated 1 h at 20 °C	82±5	56.5	49	461	2914
			54.6	733	
			56.8	980	
			64.2	360	
			70.3	385	
1 mM His no preincubation	84±6	47.9	46.1	666	2692
			48.8	775	
			52.8	448	
			63.2	427	
			69.7	377	
1 mM His preincubated 1 h at 20 °C, 10 mM NaCl added before centrifugation	86±9	56.4	48.8	494	2906
			54.2	720	
			56.9	934	
			67.0	419	
			71.0	339	

ΔH_{tot} and T_m are the heat of transition and the transition mid-point temperature of the entire endotherm. The ATPase activity is expressed as percentage of that of the native enzyme without incubation or centrifugation. Typical uncertainties arising from fitting are ±0.1° in T_d and ±4 kJ·mol^{-1} in ΔH_d. Root -mean-square deviations of the fits are typically 1–2% of the heat capacity maximum. Sample-to-sample variation in ΔH_{tot} was typically less than 4%.

3.4. Differential scanning calorimetry of pig kidney membranes

Fig. 5 shows the DSC heating scans for membranous Na,K–ATPase preparations from pig kidney under the various conditions used for the shark enzyme in Fig. 4. The thermal unfolding of the pig kidney enzyme takes place at a higher temperature than that for the shark enzyme. The heat capacity maximum occurs at ca. 54 °C for the control sample in 20 mM histidine (Fig. 5A). The shape of the denaturation endotherm of the pig kidney Na,K–ATPase also differs from that for the shark enzyme. It similarly consists of several components, but is disinguished from the endotherm of the shark enzyme by broad transitions lying at higher temperature (compare Figs. 4 and 5). Mid-point temperatures and corresponding heats of transition for the different components are listed in Table 2. Also, unlike the shark enzyme, the thermal unfolding of the pig kidney enzyme does not depend greatly on the ionic and incubation conditions. In particular, the total heat of unfolding remains the same for all four endotherms in Fig. 5 (see Table 2). This different behaviour correlates with the enhanced stability of the pig kidney enzyme that is revealed by the activity studies presented in Fig. 2. Centrifugation of the pig enzyme in 1 mM histidine did, however, shift the overall endotherm to lower temperature (compare Fig. 5C and A).

4. Discussion

The present study reveals marked differences in both thermostability and thermal unfolding between pig kidney and shark salt gland Na,K–ATPases. The activity of pig kidney enzyme is stable to higher temperatures, is less affected by centrifugation and low ionic strength, and the protein denatures at a higher temperature. For the shark enzyme, there is a clear correlation between the inactivation at low ionic strength, both by centrifugation and by elevated temperature, and the multicomponent thermal unfolding. Moderately high ionic strength (above 1 mM salt) produces stabilization that is not cation-specific, for both shark and pig kidney Na,K–ATPase.

4.1. Comparison of shark and pig Na,K–ATPase membranes

The major protein component in both pig and shark Na,K–ATPase is the α-subunit. The amino acid sequence of the shark α-subunit is 86% identical with the pig kidney sequence (93% homology) and 89% identical with that of *Torpedo californica* (94% homology), i.e., a very strong similarity between species. Fig. 6 shows the location of the 42 residues that are different between pig and shark (i.e., neither identical nor homologous), using the Ca–ATPase structure as template. In addition, there are 19 differences between pig and shark in the N-terminal part of the Na,K–ATPase α-subunit that do not map onto the Ca–ATPase. This N-terminal stretch (cf. Fig. 6) contains 37 residues for shark enzyme (30 for pig) and is the longest region with extensive differences between shark and pig sequences, which could point to a stabilizing role of this domain in the pig enzyme. It seems improbable, however, that the relatively small differences between the α-subunits of the pig and shark Na,K–ATPase alone can account for the large difference in overall melting temperature.

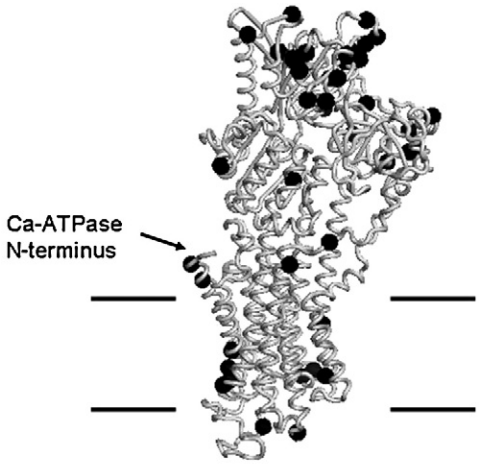


```
Shark: 1ASDKYEPAATSENATKSKKKGKKDKIDKKRDLDELKKEVSMDD43
         DKYEPAA SE+  K K K  +D  + K+       EVSMDD
Pig:   GRDKYEPAAVSEHGDKKKAKKERDMDELKK-------EVSMDD36
```

Fig. 6. Residue differences between Na,K–ATPase α-subunits from shark rectal gland and pig kidney. The Ca–ATPase structure (PDB:1t5 s) is used as a template and the positions of the 42 residues neither identical nor homologous between shark (GenBank accession number AJ781093) and pig α-subunits [37] are shown with the C–a atoms given as black spheres. The putative location of the bilayer is indicated by the horizontal lines. The sequence of the N-terminal stretch of Na,K–ATPase from shark is compared with that from pig, with identities and homologies (+) indicated. This figure was prepared using PyMOL [38].

The phospholipid composition of shark rectal gland membranes [21] shows an average unsaturation index (the number of double bonds per 100 fatty acid chains) of 210 and an average chain length of 18.1–18.6, and the phospholipid/cholesterol ratio is 1.66 mol/mol. In comparison, phospholipids from purified rabbit kidney Na,K–ATPase membranes (purified by the same methods and to the same extent as for the pig kidney enzyme) have an average unsaturation index of 115 and an average chain length of 17.4 (calculated from Tables 1 and 2 in Ref. [22], and the phospholipid/cholesterol ratio is 1.4 mol/mol (it is assumed that the lipid composition of purified rabbit kidney plasma membranes is representative of that for mammalian kidney plasma membranes). The lipid mobility in shark membranes, deduced from the ESR spectra of spin-labelled fatty acids, is considerably higher than that at the same temperature in pig kidney membranes, in agreement with the larger unsaturation index (data not shown).

The difference between the thermal stability of pig and shark enzymes could thus be related to the properties of the lipid bilayer. The higher mobility of the shark membrane lipids, at a given temperature, will lead to a more flexible (or less constrained) protein structure and thus to a higher probability of unfolding. It is notable in this connection that partial delipidation of the enzyme upon solubilization with the detergent octaethyleneglycoldodecylmonoether ($C_{12}E_8$) confers a greater thermolability. Solubilized pig kidney Na,K–ATPase aggregates readily at elevated temperatures [11], and thermal unfolding of solubilized shark enzyme occurs at a temperature 8 degrees lower than for the membrane-bound form [14]. In the latter work it was also observed that the main DSC-transition for membranous shark enzyme was lower by about 10 °C compared to kidney enzyme, in agreement with our findings (Tables 1 and 2).

4.2. Interpretation of the unfolding curves

In principle, multiple components in the overall unfolding transition could be attributed either to different steps in the unfolding pathway or to independent unfolding of different domains (or to a combination of both). The removal of different specific components by centrifugation or by incubation at elevated temperature at low ionic strength favors an interpretation in terms of domain unfolding, at least for the shark enzyme. (If autonomously unfolding domains were not involved, these components could not be removed independently.) Neither the centrifugation step nor the incubation at elevated temperatures leads to a change in the protein composition of the membranes, as evidenced by gel electrophoresis in the presence of SDS (data not shown). Because of the high thermodynamic stability of H-bonding in the hydrophobic environment of the transmembrane helices [23,24], it is expected that the principal unfolding transitions are confined largely to the extramembranous sections of the protein. It is not possible, however,

to attribute the components resolved in Tables 1 and 2 unambiguously to specific structural domains because, in spite of the high homology (see Fig. 6), the calorimetric endotherms differ considerably between shark and pig kidney enzymes. In addition, DSC thermograms of other P-type ATPases, H,K–ATPase [6] and Ca–ATPase [5], have been interpreted in terms of the unfolding of just two independent domains. Also, kinetically limited irreversible unfolding can distort the shape of the calorimetric peaks, adding uncertainty to the number of components if fitted with reversible two-state transitions [5].

Previous experiments with pig kidney Na,K–ATPase showed only three components in the unfolding transition, one of which was attributed to the β-subunit [7]. These three components have a total heat of unfolding of 1760 kJ·mol^{-1} and correspond reasonably well in position and amplitude to the three lower temperature components in Fig. 5A for pig kidney Na,K–ATPase, which together have a total heat of unfolding of 2050 kJ·mol^{-1}. In relative position and amplitude, the two components at higher temperature in Fig. 5A with a total heat of unfolding of 840 kJ·mol^{-1} resemble the second component in the unfolding endotherm of Ca–ATPase [5], which has a heat of unfolding of 380–630 kJ·mol^{-1}. The denaturation profile for pig kidney Na,K–ATPase, however, is shifted as a whole to somewhat higher temperatures than that of the Ca–ATPase.

On a mass basis, the total heat of unfolding amounts to 11.7 J/g for shark Na,K–ATPase and 17.1 J/g for the pig kidney Na,K–ATPase. Corresponding values for H,K–ATPase [6] and Ca–ATPase [5] are 7.9 and 15.5–18.0 J/g, respectively. For comparison, the mean specific unfolding enthalpy for 12 representative water-soluble proteins is 32.6±2.9 J/g [25]. The incomplete unfolding of the membrane proteins relative to the water-soluble proteins can be attributed to the stability of the transmembrane helices. Extensively proteolysed H,K–ATPase membranes exhibit no calorimetric unfolding transitions up to 80 °C [6], and we have been unable to detect calorimetric transitions in shark Na,K–ATPase membranes that were trypsinized according to the protocol of Ref. [26], which removes 50% of the extramembranous mass of the α-subunit.

4.3. Salt- and cation-induced protection against inactivation

The stabilization of the Na,K–ATPase found here is basically a non-specific effect of ionic strength, but can be enhanced by specific binding. KCl displays specificity because it offers better protection than does NaCl, TrisCl or cholineCl, whereas the three latter are equally effective and therefore contribute only the non-specific effect of ionic strength (see Fig. 3).

The ionic strength dependence of the protection afforded by Na^+, $Tris^+$ and $choline^+$ salts can be described by the Debye–Hückel theory [27]. It is assumed that the enzyme stability is modulated by mutual interactions between charged residues in the protein and possibly also by electrostatic interactions with the surrounding lipid (cf. Refs. [28,29]). The rate constant for inactivation is then given by:

$$k = k_0 e^{-\alpha\sqrt{I}} \quad (1)$$

where α is the interaction parameter of the limiting Debye–Hückel model, which applies for ionic strengths $I<0.01$ M, and k_0 is the inactivation rate constant in the absence of cations (i.e., $I=0$). The activity, A_t, measured at time t is proportional to the concentration of active enzyme remaining, hence for a first-order decay:

$$\ln\left(A_t/A_0\right) = -k_0 t e^{-\alpha\sqrt{I}} \quad (2)$$

where A_0 is the initial activity at time $t=0$. A least-squares fit of Eq. (2) to the activities at $t=20$ min for shark enzyme in solutions of NaCl is given by the lower solid line in Fig. 3A (note that at each concentration of NaCl the total ionic strength is calculated and used in the fitting procedure). This yields values of $k_0=0.27$ min^{-1} at 20 °C and $\alpha=130$. A corresponding fit for the pig kidney enzyme is given in Fig. 3B, yielding values of $k_0=0.89$ min^{-1} at 42 °C and $\alpha=210$. Within the limits of validity of the Debye–Hückel theory, the interaction parameter α is numerically equal to the sum of the products of the numbers of interacting charges that are involved in the stability of the enzyme. The relatively large values of α therefore suggest that the inactivation that is protected against by ions corresponds to a rather global electrostatic interaction involving many charged residues on the protein.

The superior protection against inactivation that is afforded by K^+ ions can be attributed to specific binding. It is well known that a K^+-occluded form of the enzyme, $E_2(K)$, is induced by micromolar concentrations of K^+ ions [30]. The binding reaction is given by $E_2+K^+ \leftrightarrow E_2(K)$, with a dissociation constant for K^+ of $K_K=[E_2]\cdot[K^+]/[E_2(K)]$. We assume for simplicity that the $E_2(K)$ form of the enzyme is fully stabilized against thermal inactivation. Loss of activity therefore occurs solely in the non-liganded E_2-form of the enzyme, which is stabilized through a non-specific effect of ionic strength (see above). The fraction of enzyme without bound K^+ is $1/(1+[K^+]/K_K)$, which is the factor by which the rate constant for inactivation is reduced by binding of K^+ ions. The activity after 20 min incubation in a solution of K^+ ions is therefore given by:

$$\ln\left(A_{t=20}/A_0\right) = -20 k_0 e^{-\alpha\sqrt{I}}/\left(1+[K^+]/K_K\right) \quad (3)$$

where I is the ionic strength of the solution which includes the contribution from the K^+ ions. A least-squares fit of Eq. (3) to the K^+-data for pig kidney enzyme is given by the upper solid line in Fig. 3B. Both k_0 and α were fixed during the fitting at the values determined from the Na^+-data. This resulted in a dissociation constant for K^+ of $K_K=13$ μM, in good agreement with that expected for induction of the $E_2(K)$-occluded form of the kidney enzyme [30]. Similar analysis of the K^+-data for the shark enzyme gave a dissociation constant of $K_K=130$ μM. The latter is somewhat larger than that expected for occlusion of K^+ by the shark enzyme, since comparable dissociation constants for K^+ with shark and kidney Na,K–ATPase are usually obtained [31]. It is possible that the assumption that the occluded enzyme does not inactivate holds less well for the shark enzyme than for the kidney enzyme. This would result in an artificially low K^+ affinity being deduced for the shark enzyme.

4.4. Correlation of inactivation and thermal unfolding

Incubation of shark Na,K–ATPase for 1 h at 20 °C under conditions of low ionic strength results in 70% loss of activity (Table 1) and the loss of components at lower temperature from the calorimetric endotherm (Fig. 4D). Relative to the control at higher ionic strength (Fig. 4A), the component at lowest temperature is lost entirely and that at next lowest temperature is reduced in amplitude (see Table 1); these components correspond to the less stable states or domains. Incubation of pig kidney Na,K–ATPase under the same conditions produces no inactivation (Table 2) and little difference in the unfolding endotherms (Fig. 5A and D). Higher ionic strength is, however, able to protect against the inactivation of the pig enzyme that occurs at 42 °C in 1 mM histidine (Fig. 2).

Centrifugation of shark Na,K–ATPase for 2 h at 4 °C under conditions of low ionic strength results in 35% loss of activity (Table 1) and the loss of components at higher temperature from the calorimetric endotherm (Fig. 4C). Relative to the control at higher ionic strength (Fig. 4A), the component with T_d=45.1 °C preceeding the highest temperature peak is lost entirely, which accounts almost completely for the total decrease in heat of unfolding of 630 kJ·mol^{-1} (see Table 1). Centrifugation of pig kidney Na,K–ATPase under the same conditions produces no inactivation (Table 2) but a marked change in the unfolding endotherms (Fig. 5A and C). Components of the endotherm at lower and intermediate temperatures are shifted to lower temperature and heat is lost from the intermediate component. This destabilization does not, however, lead to a decrease in overall heat of unfolding.

Monovalent chloride salts are therefore able to stabilize the Na,K–ATPase in at least two distinct ways because centrifugation and high-temperature incubation at low ionic strength have very different effects on thermal unfolding.

4.5. Comparison with other studies

Exposure to proteases and kinases has been investigated after heating kidney Na,K–ATPase to 55 °C [12,13], a temperature within the thermal unfolding transition (see Fig. 5 and Ref. [7]). Incubation of pig [13] or rat [12] kidney enzyme for 30 min at 55 °C causes unfolding of the extracellular part of the β-subunit with retention in the membrane, and extrusion of up to three transmembrane spans (M8–M10) and the C-terminus of the α-subunit at the extracellular side of the membrane. Subsequent studies [32] showed that the γ-subunit is also lost from the membrane. This reorganization of the intramembrane domain may account partly for the higher heat of unfolding of the Na,K–ATPase from pig kidney relative to that from shark salt gland (see Tables 1 and 2). Interesting also in this context is the finding that the β-subunit of kidney Na,K–ATPase can be cleaved proteolytically [12,13] whereas that of the shark enzyme is completely resistant to trypsin [26].

SERCA1a Ca–ATPase, which has a single subunit, loses 60% of its activity after 120 min at 41 °C [33], whereas kidney Na,K–ATPase is completely stable over this period at 42 °C when in the presence of ions (see Fig. 2). This suggests that part of the enhanced stability of Na,K–ATPase might arise from interactions between subunits. Indeed, renal Na,K–ATPase from mice lacking the γ-subunit (FXYD2) gene is found to exhibit increased thermal lability [34]. Additionally, the γ-subunit (FXYD10) from shark Na,K–ATPase [35] interacts differently with the α-subunit and is more sensitive to proteolysis by trypsin than is that from kidney [36], suggesting a looser interaction between subunits for the former. This difference in strength of intersubunit associations, possibly mediated by lipid–protein interactions, could contribute to the lower thermostability of the shark enzyme.

In conclusion we have shown that Na,K–ATPase from a warm-blooded animal (the pig) is much more stable towards thermal denaturation than Na,K–ATPase from the cold-blooded shark, and that enzymatic stability and structural stability is correlated. In addition we find that stabilization is very ionic strength dependent for both types of enzyme, with protection requiring only a few millimolars of monovalent chloride salts.

Acknowledgments

We thank Ms. Angelina Damgaard and Ms. Birthe Bjerring Jensen (Aarhus), and Ms. Erika Konya (Szeged) for their excellent technical assistance. Elfrieda Fodor was a recipient of a Bolyai research fellowship from the Hungarian Academy of Sciences. Financial support from the Danish Medical Research Council (grant no. 52-00-914), the Novo Nordisk Foundation and the Hungarian Scientific Research Fund (OTKA T043425 and K68804) is gratefully acknowledged.

References

[1] J.H. Kaplan, Biochemistry of Na,K–ATPase, Annu. Rev. Biochem. 71 (2002) 511–535.
[2] A.G. Therien, H.X. Pu, S.J.D. Karlish, R. Blostein, Molecular and functional studies of the gamma subunit of the sodium pump, J. Bioenerg. Biomemb. 33 (2001) 407–414.
[3] C. Toyoshima, G. Inesi, Structural basis of the ion pumping by Ca^{2+}–ATPase of the sarcoplasmatic reticulum, Annu. Rev. Biophys. Chem. 73 (2004) 269–292.
[4] H. Hebert, P. Purhonen, H. Vorum, K. Thomsen, A.B. Maunsbach, Three-dimensional structure of renal Na,K–ATPase from cryo-electron microscopy of two-dimensional crystals, J. Mol. Biol. 314 (2001) 479–494.
[5] J.R. Lepock, A.M. Rodahl, C. Zhang, M.L. Heynen, B. Waters, K.-H. Cheng, Thermal denaturation of the Ca^{2+}–ATPase of sarcoplasmic reticulum reveals two thermodynamically independent domains, Biochemistry 29 (1990) 681–689.
[6] M. Gasset, J. Laynez, M. Menendez, V. Raussens, E. Goormaghtigh, Structural domain organization of gastric H^+, K^+–ATPase and its rearrangement during the catalytic cycle, J. Biol. Chem. 272 (1997) 1608–1614.
[7] A.V. Grinberg, N.M. Gevondyan, N.V. Grinberg, V.Y. Grinberg, The thermal unfolding and domain structure of Na^+/K^+-exchanging ATPase. A scanning calorimetry study, Eur. J. Biochem. 268 (2001) 5027–5036.
[8] J.V. Møller, B. Juul, M. LeMaire, Structural organization, ion transport, and energy transduction of P-type ATPases, Biochim. Biophys. Acta 1286 (1996) 1–51.
[9] J.V. Møller, P. Nissen, T.L.-M. Sørensen, M. LeMaire, Transport mechanism of the sarcoplasmic reticulum Ca^{2+}–ATPase pump, Curr. Opin. Struct. Biol. 15 (2005) 387–393.
[10] T.H. Fischer, The effect of Na^+ and K^+ on the thermal denaturation of Na^++K^+-dependent ATPase, Biochem. J. 211 (1983) 771–774.
[11] P.L. Jørgensen, J.P. Andersen, Thermoinactivation and aggregation of αβ units in soluble and membrane-bound (Na,K)–ATPase, Biochemistry 25 (1986) 2889–2897.

[12] E. Arystarkhova, D.L. Gibbons, K.J. Sweadner, Topology of the Na,K–ATPase. Evidence for externalization of a labile transmembrane structure during heating, J. Biol. Chem. 270 (1995) 8785–8796.
[13] R. Goldshleger, D.M. Tal, S.J.D. Karlish, Topology of the α-subunit of Na, K–ATPase based on proteolysis. Lability of the topological organization, Biochemistry 34 (1995) 8668–8679.
[14] M. Stolz, E. Lewitzki, E. Schick, M. Mutz, E. Grell, Calorimetry of Na,K–ATPase, Ann. N.Y. Acad. Sci. 986 (2003) 245–246.
[15] M. Esmann, N.U. Fedosova, A.B. Maunsbach, Protonation-dependent inactivation of Na,K–ATPase by hydrostatic pressure developed at high-speed centrifugation, Biochim. Biophys. Acta 1468 (2000) 320–328.
[16] J.C. Skou, M. Esmann, Preparation of membrane-bound and of solubilized ($Na^+ + K^+$)–ATPase from rectal glands of *Squalus acanthias*. The effect of preparative procedures on purity, specific and molar activity, Biochim. Biophys. Acta 567 (1979) 436–444.
[17] P.L. Jørgensen, Purification and characterization of ($Na^+ + K^+$)–ATPase. III. Purification from the outer medulla of mammalian kidney after selective removal of membrane components by sodium dodecyl sulphate, Biochim. Biophys. Acta 356 (1974) 36–52.
[18] I. Klodos, M. Esmann, R.L. Post, Large-scale preparation of sodium–potassium ATPase from kidney outer medulla, Kidney Int. 62 (2002) 2097–2100.
[19] M. Esmann, ATPase and phosphatase activity of Na^+,K^+–ATPase: molar and specific activity, protein determination, Methods Enzymol. 156 (1988) 105–115.
[20] C.H. Fiske, Y. Subbarow, The colorimetric determination of phosphorus, J. Biol. Chem. 66 (1925) 375–400.
[21] F. Cornelius, N. Turner, H.R.Z. Christensen, Modulation of Na,K–ATPase by phospholipids and cholesterol. II. Steady-state and presteady-state kinetics, Biochemistry 42 (2003) 8541–8549.
[22] W.H.M. Peters, A.M.M. Fleuren-Jakobs, J.J.H.H.M. de Pont, S.L. Bonting, Studies on ($Na^+ + K^+$)–activated ATPase. XLIX. Content and role of cholesterol and other neutral lipids in highly purified rabbit kidney enzyme preparation, Biochim. Biophys. Acta 649 (1981) 541–549.
[23] J.-L. Popot, D.M. Engelman, Membrane protein folding and oligomerization — the 2-stage model, Biochemistry 29 (1990) 4031–4037.
[24] T. Haltia, E. Freire, Forces and factors that contribute to the structural stability of membrane proteins, Biochim. Biophys. Acta 1228 (1995) 1–27.
[25] T. Haltia, N. Semo, J.L.R. Arrondo, F.M. Goni, E. Freire, Thermodynamic and structural stability of cytochrome *c* oxidase from *Paracoccus denitrificans*, Biochemistry 33 (1994) 9731–9740.
[26] M. Esmann, A. Arora, A.B. Maunsbach, D. Marsh, Structural characterization of Na,K–ATPase from shark rectal glands by extensive trypsinization, Biochemistry 45 (2006) 954–963.
[27] R.A. Robinson, R.H. Stokes, Electrolyte solutions, (second edition), Butterworth, London, 1986, p. 571.
[28] M. Esmann, D. Marsh, Spin label studies on the origin of the specificity of lipid–protein interactions in Na,K–ATPase membranes from *Squalus acanthias*, Biochemistry 24 (1985) 3572–3578.
[29] M. Esmann, D. Marsh, Lipid–protein interactions with the Na,K–ATPase, Chem. Phys. Lipids 141 (2006) 94–104.
[30] I.M. Glynn, S.J.D. Karlish, Occluded cations in active transport, Annu. Rev. Biochem. 59 (1990) 171–205.
[31] L.O. Jakobsen, Structural Studies of Cation and Nucleotide Binding Sites in Na,K–ATPase, PhD Dissertation, The Faculty of Health Sciences, University of Aarhus, Denmark (2004).
[32] C. Donnet, E. Arystarkhova, K.J. Sweadner, Thermal denaturation of the Na,K–ATPase provides evidence for α–α oligomeric interaction and γ subunit association with the C-terminal domain, J. Biol. Chem. 276 (2001) 7357–7365.
[33] A.R. Tupling, A.O. Gramolini, T.A. Duhamel, H. Kondo, M. Asahi, S.C. Tsuchiya, M.J. Borrelli, J.R. Lepock, K. Otsu, M. Hori, D.H. MacLennan, H.J. Green, HSP70 binds to the fast-twitch skeletal muscle sarco(endo)plasmic reticulum Ca^{2+}–ATPase (SERCA1a) and prevents thermal inactivation, J. Biol. Chem. 279 (2004) 52382–52389.
[34] D.H. Jones, T.Y. Li, E. Arystarkhova, K.J. Barr, R.K. Wetzel, J. Peng, K. Markham, K.J. Sweadner, G.-H. Fong, G.M. Kidder, Na,K–ATPase from mice lacking the γ subunit (FXYD2) exhibits altered Na^+ affinity and decreased thermal stability, J. Biol. Chem. 280 (2005) 19003–19011.
[35] Y.A. Mahmmoud, H. Vorum, F. Cornelius, Interaction of FXYD10 (PLMS) with Na,K–ATPase from shark rectal glands — close proximity of Cys^{74} of FXYD10 to Cys^{254} in the A domain of the α-subunit revealed by intermolecular thiol cross-linking, J. Biol. Chem. 280 (2006) 27776–27782.
[36] M. Füzesi, K.-E. Gottschalk, M. Lindzen, A. Shainskaya, B. Küster, H. Garty, S.J.D. Karlish, Covalent cross-links between the γ-subunit (FXYD2) and α and β subunits of Na,K–ATPase — modelling the α–γ interaction, J. Biol. Chem. 280 (2005) 18291–18301.
[37] Y.A. Ovchinnikov, N.N. Modyanov, N.E. Broude, K.E. Petrukhin, A.V. Grishin, N.M. Arzamazova, N.A. Aldanova, G.S. Monastyrskaya, E.D. Sverdlov, Pig kidney Na^+,K^+–ATPase. Primary structure and spatial organization, FEBS Lett. 201 (1986) 237–245.
[38] W.L. Delano, PyMOL molecular graphics system, http://www.pymol.sourceforge.net2002(online).